MASS TRANSFER CYCLES IN CLOSE BINARIES WITH EVOLVED COMPANIONS

A. R. King, [1], J. Frank, [2] U. Kolb [1] and H. Ritter [3]

ABSTRACT

We give a global analysis of mass transfer variations in low-mass X-ray binaries and cataclysmic variables whose evolution is driven by the nuclear expansion of the secondary star. We show that limit cycles caused by irradiation of the secondary by the accreting primary are possible in a large class of these binaries. In the high state the companion transfers a large fraction of its envelope mass on a thermal timescale. In most cases this implies super–Eddington transfer rates, and would thus probably lead to common–envelope evolution and the formation of an ultrashort–period binary. Observed systems with (sub)giant secondaries stabilize themselves against this possibility either by being transient, or by shielding the secondary from irradiation in some way.

Subject headings: accretion — instabilities — stars: binaries: close — stars: cataclysmic variables —

1. INTRODUCTION

Semidetached binaries in which a compact object (white dwarf, neutron star or black hole) accretes material via Roche lobe overflow from a companion on or near the main sequence are of great interest in current astrophysics. The evolution of such systems is driven by orbital angular momentum losses via gravitational radiation and magnetic braking (see e.g. King 1988 for a review). Thus most properties of the binary, particularly the mean mass transfer rate, depend essentially only on the secondary mass M_2 and change on the timescale $t_J \sim 10^8 - 10^9$ yr for angular momentum loss. In a recent paper (King, Frank, Kolb & Ritter 1996a, henceforth Paper I) we discussed the conditions under which mass transfer can vary cyclically about the evolutionary mean in these systems by developing a general formalism allowing one to study the stability of mass transfer in systems driven by angular momentum losses. The existence of cycles is required to

[1]Astronomy Group, University of Leicester, Leicester LE1 7RH, U.K. (ark@star.le.ac.uk, uck@star.le.ac.uk)

[2]Department of Physics and Astronomy, Louisiana State University, Baton Rouge, LA 70803-4001, USA (frank@rouge.phys.lsu.edu)

[3]Max–Planck–Institut für Astrophysik, Karl–Schwarzschild–Str. 1, D 85748 Garching, Germany (hsr@MPA-Garching.MPG.DE)

account for the wide dispersion of e.g. mass transfer rates at a given orbital period. We concluded that the most likely cause of such cycles is weak irradiation of the companion star by the accreting component. The conditions for this appear to be fulfilled in a large class of cataclysmic variables (CVs), in which the accreting star is a white dwarf.

Of course semidetached evolution is not restricted to systems with main–sequence companions. In systems with orbital periods $P \gtrsim 1$ day the orbital evolution and hence the rate of mass transfer is either determined or strongly influenced by nuclear evolution of the companion. In this paper we discuss the stability of mass transfer in systems containing a giant or a subgiant companion and consider the possibility of irradiation–driven mass transfer cycles similar to those thought to exist in CVs. For this purpose we generalize the analysis of Paper I to include the effects of nuclear evolution on the radius variations by using a simple core–envelope model for the companion. This is a good representation of systems with low–mass giant secondaries, which constitute the great majority of long–period compact binaries. However this description does not apply to the recently–discovered black–hole transient GRO J1655-40, where the companion star appears to be crossing the Hertzsprung gap (Orosz & Bailyn, 1996).

2. GLOBAL ANALYSIS OF MASS TRANSFER VARIATIONS

In this section we follow closely the formalism developed in Paper I, casting the equations governing time–dependent mass transfer in a semidetached binary in a form suitable for global analysis including the effects of nuclear evolution. We restrict our analysis to the effect of variations in the radius R_2 of the lobe–filling star on the transfer rate, as this is the simplest way of causing mass transfer variations (other ways can easily be accomodated: Paper I gives an example). Note that this part of the analysis is quite general, in that there is no presumption at this point that the radius variations result from irradiation.

Radius changes can result from dynamical, thermal or secular processes. For example, local adjustments in the structure of the atmospheric layers can take place on the shortest (dynamical) timescale, while adjustments of the stellar radius in response to secular mass loss and nuclear evolution occur on the longest (secular) driving timescale $t_{\rm dr}$ defined more precisely below. We represent the radius variation as

$$\frac{\dot{R}_2}{R_2} = \zeta_s \frac{\dot{M}_2}{M_2} + K_{\rm th}(R_2, \dot{M}_2) + K_{\rm nuc} \ . \qquad (1)$$

Here ζ_s is the adiabatic mass–radius exponent ($\simeq -1/3$ for a fully convective star), $K_{\rm th}(R_2, \dot{M}_2)$ represents radius variations due to thermal relaxation and irradiation of the star by the primary, and $K_{\rm nuc} = (\partial \ln R_2/\partial t)_{\rm nuc}$ represents the secular changes due to nuclear evolution. We considered examples of specific forms of $K(R_2, \dot{M}_2)$ in Paper I and will discuss these again later. The change

of the mass transfer rate is given by

$$\ddot{M}_2 = \frac{\dot{M}_2}{H}(\dot{R}_2 - \dot{R}_\mathrm{L}) \approx \dot{M}_2 \frac{R_2}{H}\left(\frac{\dot{R}_2}{R_2} - \frac{\dot{R}_\mathrm{L}}{R_\mathrm{L}}\right) , \tag{2}$$

where R_L is the critical Roche radius, and H is the pressure scale height in the secondary star's atmosphere. The approximation given by (2) is justified since even for giant companions $|R_2 - R_\mathrm{L}| << R_\mathrm{L}, R_2$. The response of the Roche radius to mass loss is described by

$$\frac{\dot{R}_\mathrm{L}}{R_\mathrm{L}} = \zeta_\mathrm{R} \frac{\dot{M}_2}{M_2} + 2\frac{\dot{J}}{J} , \tag{3}$$

where ζ_R is a function of the mass ratio M_2/M_1, approximately given by $\zeta_\mathrm{R} \approx 2M_2/M_1 - 5/3$ for conservative mass transfer, and $\dot{J}$ is the rate of loss of orbital angular momentum. Inserting (1) and (3) into (2), we obtain

$$\ddot{M}_2 = \dot{M}_2 \frac{R_2}{H}\left[(\zeta_s - \zeta_\mathrm{R})\frac{\dot{M}_2}{M_2} + K_\mathrm{th} + K_\mathrm{nuc} - 2\frac{\dot{J}}{J}\right] . \tag{4}$$

For the more general case considered here the evolution of the binary is driven by the combined effects of nuclear evolution and angular momentum losses. We introduce the effective driving timescale t_dr, as follows,

$$\frac{1}{t_\mathrm{dr}} = \frac{1}{t_\mathrm{nuc}} + \frac{2}{t_J} , \tag{5}$$

where $t_\mathrm{nuc} = K_\mathrm{nuc}^{-1}$ is the nuclear timescale, and $t_J = -J/\dot{J}$ is the timescale for angular momentum losses. The nuclear timescale is a strong function of the core mass, and is $\sim 10^7 - 10^9$ yr for giants and much longer for low mass main sequence dwarfs. The angular momentum loss time scale t_J is typically $\sim 10^8 - 10^9$ yr for main sequence companions, but could be much longer for evolved companions. Thus orbital evolution is driven mainly by angular momentum losses in systems with main sequence companions (e.g. CVs) and nuclear processes in systems with evolved companions. The introduction of t_dr allows us to treat both cases simultaneously. We define a dimensionless mass transfer rate

$$x = \frac{-\dot{M}_2}{(-\dot{M}_2)_\mathrm{ad}} = -\frac{\dot{M}_2}{M_2}(\zeta_s - \zeta_\mathrm{R})t_\mathrm{dr} , \tag{6}$$

where $(-\dot{M}_2)_\mathrm{ad}$ is the adiabatic mass transfer rate i.e. the steady rate implied by equation (4) with $K_\mathrm{th} = 0$. A system undergoing stable mass transfer will typically do so at $x \sim 1$ (see Sect. 3). We also introduce the dimensionless stellar radius

$$r = R_2/R_e \ , \tag{7}$$

where $R_e = R_e(M_2, M_c)$ is the radius of the secondary in thermal equilibrium for a given total mass M_2 and a core mass M_c. The radii and luminosities of lower giant–branch stars are virtually independent of the mass of the envelope but depend strongly on the mass of the degenerate helium core (Refsdal & Weigert 1970). We allow R_e formally to depend on the total mass because then the equations obtained are identical in form to those derived in Paper I and have wider applicability.

As we discuss in Sect. 3, the secular equilibrium radius of the companion under stable mass transfer differs slightly from R_e. Although the equilibrium radius R_e is only attained in the absence of mass transfer, we write formally

$$\frac{\dot{R}_e}{R_e} = \zeta_e \frac{\dot{M}_2}{M_2} + K_{\rm nuc} \ , \tag{8}$$

where ζ_e is defined by the above equation. Taking the time derivative of equation (6), and neglecting secular variations of H, we obtain

$$-\ddot{M}_2 = \frac{M_2}{(\zeta_s - \zeta_{\rm R})t_{\rm dr}}\dot{x} + \frac{\dot{M}_2 x}{(\zeta_s - \zeta_{\rm R})t_{\rm dr}} + \dot{M}_2 \frac{{\rm d}\ln\left[(\zeta_s - \zeta_{\rm R})t_{\rm dr}\right]}{{\rm d}t} \ . \tag{9}$$

Finally, we introduce $\epsilon = H/R_e$, which is typically $\simeq 10^{-3}$ for lower giant branch stars (see below). We define the dimensionless thermal relaxation function $p(r,x) = K_{\rm th}t_{\rm dr}$, and the dimensionless time $\tau = t/(\epsilon t_{\rm dr})$. With these assumptions and definitions (9) becomes

$$\frac{{\rm d}x}{{\rm d}\tau} = rx[1 + p(r,x) - x] + \epsilon x\left[\frac{x}{(\zeta_s - \zeta_{\rm R})} + t_{\rm dr}\frac{{\rm d}\ln\left[(\zeta_s - \zeta_{\rm R})t_{\rm dr}\right]}{{\rm d}t}\right] \ . \tag{10}$$

Note that since the terms inside the second set of square brackets are of order unity and are multiplied by ϵ, they can be safely neglected. Thus (10) reduces to

$$\frac{{\rm d}x}{{\rm d}\tau} = rx[1 + p(r,x) - x] \ . \tag{11}$$

With the variations of the equilibrium radius given by equation (8), and using the above conventions, the radius equation (1) becomes

$$\frac{{\rm d}r}{{\rm d}\tau} = \epsilon r\left[p(r,x) - \frac{x}{\lambda}\right] \ , \tag{12}$$

where $\lambda = (\zeta_s - \zeta_{\rm R})/(\zeta_s - \zeta_e)$. The equations (11, 12) describing radius and mass transfer variations are identical in form to those derived in Paper I. Thus we can take over from Paper I all the results

for the phase plane motion of the system, the critical curves $\dot{r} = 0$, $\dot{x} = 0$, the fixed point(s) (r_0, x_0) at the intersection(s) of these critical curves, the stability anaylsis for the fixed point(s), and the conditions for limit cycles, with the modification that now $t_{\rm dr}$ is a more general driving time which includes both systemic angular momentum losses and nuclear evolution. In the limit $t_{\rm nuc} \to \infty$ we recover the case studied in Paper I.

From equations (11, 12) it is easy to see that the stationary (secular mean) mass transfer rate at the fixed point $x_0 = (\zeta_s - \zeta_{\rm R})/(\zeta_e - \zeta_{\rm R})$ depends on the properties of the companion and the driving rate. In particular it is independent of $p(r, x)$ (as it must be); and in most realistic cases $x_0 \sim 1$. The radius r_0 at the fixed point on the other hand is given implicitly in terms of $p(r, x)$; again we typically have $r_0 \sim 1$ (see Paper I for further details).

3. BINARIES WITH SUBGIANT AND GIANT COMPANIONS

In their study of the evolution of compact binaries containing a lower giant branch companion, Webbink, Rappaport and Savonije (1983) introduced simple analytic expressions for the luminosity and radius in terms of the core mass. For our purposes it suffices to take only the first two terms of their approximate formulae for the radius

$$R_e(M_c) = 12.55{\rm R}_\odot \left(\frac{M_c}{0.25{\rm M}_\odot} \right)^{5.1} , \tag{13}$$

and the luminosity

$$L_e(M_c) = 33.1{\rm L}_\odot \left(\frac{M_c}{0.25{\rm M}_\odot} \right)^{8.1} , \tag{14}$$

in thermal equilibrium. Using these equations we can readily estimate ϵ for these stars

$$\epsilon = \frac{H}{R_e} = 2.1 \times 10^{-3} \mu^{-1} \left(\frac{M_c}{0.25{\rm M}_\odot} \right)^{4.6} \left(\frac{M_2}{{\rm M}_\odot} \right)^{-1} , \tag{15}$$

where μ is the mean molecular weight in the stellar atmosphere. From (13, 14) the nuclear timescale for radial variations is $t_{\rm nuc} = M_c/(5.1\dot{M}_c)$, where $\dot{M}_c$ is calculated from the equilibrium luminosity assuming a hydrogen mass fraction of 0.7 and an energy yield of 6×10^{18} erg g^{-1}. Thus

$$t_{\rm nuc} = 1.0 \times 10^8 {\rm yr} \left(\frac{M_c}{0.25{\rm M}_\odot} \right)^{-7.1} , \tag{16}$$

The Kelvin-Helmholtz timescale is defined for the whole star as $t_{\rm KH} = GM_2^2/(R_e L_e)$ so

$$t_{\rm KH} = 7.6 \times 10^4 {\rm yr} \left(\frac{M_2}{{\rm M}_\odot} \right)^2 \left(\frac{M_c}{0.25{\rm M}_\odot} \right)^{-13.2} . \tag{17}$$

The ratio of these timescales plays a major role in the discussion of thermal relaxation and stability. We define

$$\rho_{\rm nuc} = \frac{t_{\rm nuc}}{t_{\rm KH}} = 1.4 \times 10^3 \left(\frac{M_2}{{\rm M}_\odot} \right)^{-2} \left(\frac{M_c}{0.25{\rm M}_\odot} \right)^{6.1} . \tag{18}$$

Since no explicit dependence of R_e on the total mass of the companion M_2 is allowed in equations (13, 14), it appears that $\zeta_e = 0$. However, both computed models of lower giant branch stars and analytic treatment of nearly fully convective stars following the approximations used by Kippenhahn and Weigert (1990) for the Hayashi line show a weak dependence on the total stellar mass M_2. Taking a photospheric opacity of the form $\kappa = \kappa_0 P^a T^b$, and adopting a polytropic index $n = 3/2$ for the envelope, one can show that

$$\zeta_e = -\frac{a+3}{5.5a+b+1.5} \ . \tag{19}$$

With $a = 1$, $b = 3$, the above expression yields $\zeta_e = -0.4$, while direct estimates from numerical stellar models indicate $\zeta_e \approx -0.2$ to -0.3. We adopt the latter range in describing the reaction of the star to mass loss, although the relation (13) is adequate for computing the nuclear and thermal timescales.

We now describe the effects of thermal relaxation and irradiation on the radius of the evolved companion. We do this here using a simple homologous model and making the same approximations as in King et al. 1995 and in Paper I with slight changes appropriate for giants:

1) Homology relations can be used to describe the stellar structure, i.e. the effective temperature T_* on the unirradiated portion of the stellar surface remains essentially constant (Hayashi line) and any stellar radius change changes the surface luminosity as $L \propto R_2^2$. In constrast $L_{\rm nuc}$ remains unchanged, as given by equation (14).

2) If a fraction s of the stellar surface is exposed to a uniform irradiating flux F, the luminosity of the star, i.e. the loss of energy per unit time from the interior, is reduced by the blocking luminosity

$$L_b = sL \ \tanh\left\{k\,\frac{F}{F_*}\right\} \ , \tag{20}$$

where $F_* = \sigma T_*^4$ is the unperturbed stellar flux and k a parameter which is adjusted to approximate the results of more realistic model calculations [e.g. those by Ritter et al. (1996a, 1996b)]. The above ansatz for L_b is motivated by the facts that a) $L_b = 0$ if $F = 0$, b) $L_b \to sL$ if $F \gg F_*$, and c) the transition between $F = 0$ and $F \gg F_*$ is smooth and monotonic. With these assumptions we get the thermal relaxation function including irradiation effects (cf. equation (8) of King et al. 1995 and equation (38) of Paper I)

$$p(r,x) = -f\rho\,\left\{\left[1 - s\,\tanh\left(\frac{x}{x_c}\right)\right]\,r^3 - r\right\} \ . \tag{21}$$

Note that the quantity $\rho = t_{\rm dr}/t_{\rm KH}$ introduced above differs from $\rho = t_J/t_{\rm KH}$ used in Paper I [see equation (5)]. The ratio $f = t_{\rm KH}/t_{\rm ce}$, with $t_{\rm ce}$ being the thermal timescale for the convective envelope, is a constant which depends on the internal structure (i.e. mainly on the ratio of envelope mass to the total mass of the secondary), and

$$x_c = \frac{2(\zeta_s - \zeta_{\rm R})\rho}{k\eta}\,\frac{M_2}{M_1}\,\frac{R_1}{R_e}\,\left(\frac{a}{R_e}\right)^2 . \tag{22}$$

This is the dimensionless critical mass transfer rate which yields an irradiating flux $F = F_*/k$. Cycles typically occur provided that x_c is $\lesssim$ the secular mean transfer rate x_0. In (22) a is the orbital separation and η a dimensionless efficiency factor relating the irradiating flux F to the mass transfer rate via

$$F = \frac{\eta}{8\pi} \frac{GM_1(-\dot{M}_2)}{R_1 a^2} \ . \tag{23}$$

The critical mass transfer rate for CVs is $x_c \sim 0.1\rho/k\eta \sim 1 - 10$, where the value of k depends on the type of companion star assumed, while η depends mainly on the radiation spectrum (typical values are $0.1 \lesssim \rho \lesssim 5, 0.2 \lesssim k \lesssim 0.9$, with $\eta \sim$ a few percent). As this critical rate is of order the secular mean mass transfer rate $x_0 \sim 1$, irradiation can potentially drive cycles in CVs, as we found in paper I. For LMXBs with similar mass ratios, the much smaller neutron star or effective black–hole radius implies $x_c \sim 0.0001\rho/k\eta \sim 0.1 - 1$. Thus we can potentially expect cycles in these systems also. This contrasts with the case of LMXBs with unevolved companions (cf Paper I), where the companion is too strongly irradiated to give cycles (critical transfer rates $x_c << x_0 \sim 1$). For LMXBs with evolved companions the large ratio ρ of driving to thermal timescales almost compensates the effect of the smaller primary radius to give $x_c \sim 0.1 - 1$.

4. STABILITY OF MASS TRANSFER FROM AN EVOLVED COMPANION

The simple thermal relaxation function given in the previous section allows us to discuss the stability of mass transfer in close binaries with evolved companions. More detailed calculations using the bipolytrope approximation (Ritter, Zhang & Kolb 1996b) or integrating the full equations of stellar structure with appropriate changes in the boundary conditions (Hameury & Ritter 1996) produce results which to a first approximation can be represented by this analytic form with suitable $k, x_c \sim 1$. In Paper I we noted that a necessary condition for limit cycles is that the fixed point is unstable, which in turn requires $p_r < 0$ and $p_x > 1$ simultaneously. These derivatives are easily calculable for the simple form of equation (21), namely

$$p_r(r_0, x_0) = -f\rho \left\{ \left[1 - s \tanh\left(\frac{x_0}{x_c}\right) \right] 3r_0^2 - 1 \right\} \ , \tag{24}$$

and

$$p_x(r_0, x_0) = \frac{f\rho s}{x_c} r_0^3 \mathrm{sech}^2\left(\frac{x_0}{x_c}\right) \ . \tag{25}$$

For physically reasonable situations $s < 0.5$ and $r_0 > 1$, and thus clearly $p_r < 0$ as required. The second condition $p_x > 1$ for instability can be rewritten as in Paper I:

$$s\frac{x_0}{x_c}\mathrm{sech}^2\left(\frac{x_0}{x_c}\right) > \frac{x_0}{f\rho r_0^3} \ , \tag{26}$$

where the l.h.s. is a function which has a maximum value of $\approx 0.448s$ at $x_0/x_c \approx 0.78$ and vanishes at both small and large x_0/x_c. As emphasised in Paper I the r.h.s. of equation (26) depends mainly

on the type of companion and the driving mechanism. Clearly the large values of ρ for giant or subgiant companions makes these systems extremely vulnerable to the irradiation instability. Note that if $s = 0$ in (26), i.e. irradiation is not included, or the flux is somehow blocked (e.g. by a thick disk), the inequality is violated and mass transfer driven by nuclear evolution is stable as assumed in conventional treatments of these systems.

Thus the simple model described above suggests that most binaries with irradiated lower giant branch–companions cannot transfer mass at a stable rate. More detailed models discussed later confirm this result. While the linearized equations are adequate to discuss the stability of the fixed point, as in Paper I, we need the full non-linear evolution equations to understand the ultimate fate of the system. It turns out that the phase point representing the evolution of the system away from an unstable fixed point is trapped in its vicinity, and will settle into a limit cycle which is described in more detail below.

5. PROPERTIES OF THE LIMIT CYCLE

The simple thermal relaxation functions $p(r,x)$ given by (21) for evolved companions and equation (38) of Paper I for main sequence companions yield approximate analytic expressions for a number of properties of the limit cycle. The two cases can be treated simultaneously by taking

$$p(r,x) = -f\rho \left\{ \left[1 - s \tanh\left(\frac{x}{x_c}\right)\right] r^3 - r^{-(\nu+2)} \right\} , \tag{27}$$

with ρ as defined in this paper, and $\nu = 5 - 6$ or $\nu = -3$ for main sequence and giant companions respectively. Some of the results given below depend on having $\rho >> 1$, which is satisfied very well by giants [for which $\rho \approx \rho_{\rm nuc}$, see (18)] but not always by main–sequence companions. Nevertheless, since most of the analytic results described below can also be obtained for main–sequence companions, we shall quote them here too.

From (11) the critical curve $\dot{x} = 0$ is given by $1 + p(r,x) - x = 0$. The chosen form of $p(r,x)$ gives two branches of this curve with different slopes: a low branch with $x << x_c$ and a high branch where $x >> x_c$. For the low branch one can easily show using the approximation $\tanh(x/x_c) \approx x/x_c$ that

$$x_L \approx \frac{f\rho(r^3 - r^{-\nu-2}) - 1}{f\rho s r^3/x_c - 1} . \tag{28}$$

The denominator in the above equation can be rewritten using (25) as $p_x \cosh^2(x/x_c) - 1$. The condition $p_x > 1$ for instability ensures that this denominator is positive near x_0; as x_L must be finite the denominator must remain positive everywhere on the lower branch, implying a positive slope there. Since in general the radial variations are small departures from equilibrium, we can linearize around $r = 1$ to get $x_L = 0$ at $r = 1 + 1/[f\rho(5+\nu)]$. In general the slope of this critical curve is given by

$$\left(\frac{{\rm d}x}{{\rm d}r}\right)_{\dot{x}=0} = \frac{-p_r}{p_x - 1} , \tag{29}$$

where $p_r < 0$ for physically relevant cases. If $f\rho >> 1$, as in the case of evolved companions, then the slope of the lower branch at $x = 0$ is approximately $(5+\nu)x_c/s$.

The upper branch is obtained by setting the tanh factor to unity and thus

$$x_U \approx 1 + f\rho s r^3 - f\rho(r^3 - r^{-\nu-2}) \ . \tag{30}$$

For small departures from the equilibrium radius this reduces to $x = 1+f\rho s - f\rho(5+\nu-3s)(r-1)$ showing that the upper branch has a large negative slope and is therefore stable (as $s < 0.5$ we have $(5+\nu-3s) > 3.5+\nu$, which is > 0.5 even for giant companions with $\nu = -3$). At some intermediate value of the transfer rate x_t there is a turning point at which $(\mathrm{d}r/\mathrm{d}x)_{\dot{x}=0} = 0$, or equivalently where $p_x = 1$. This turning point therefore satisfies the equation

$$\cosh^2\left(\frac{x_t}{x_c}\right) = \frac{sf\rho r_t^3}{x_c} \ , \tag{31}$$

where r_t is the dimensionless radius at the turning point. In general r_t and x_t must be obtained by solving equation (31) together with $1 + p(r,x) - x = 0$, which can be easily done iteratively. Note also that as in Paper I, the axis $x = 0$ is formally part of the $\dot{x} = 0$ curve, although it takes infinite time to reduce x to zero (see Fig. 1). From the considerations above we can see that the fixed point is unstable when $x_t > x_0 > 0$.

The maximum expansion stage of the secondary is reached close to r_t. We could estimate r_t by asking for the radius at which $x_L = x_U$, but we prefer to use a physical argument based on the assumptions made in the model: the maximum expansion of the companion is reached when all the luminosity generated is emitted by the unilluminated side at the unperturbed effective temperature. This yields $p(r_t, x_t) \approx 0$ and

$$r_t \approx (1 - s_{\rm eff})^{-1/(\nu+5)} \approx 1 + \frac{s_{\rm eff}}{\nu+5} \ , \tag{32}$$

where $s_{\rm eff} = s\tanh(x_t/x_c) \sim s$. Formally if $p(r,x) = 0$ for non–vanishing illumination we again get the adiabatic mass transfer rate $x = 1$ and thus $\dot{x} = 0$. This simple argument shows that main sequence companions expand relatively little under illumination while giants expand substantially: in general we have $r_t \sim 1+0.1s_{\rm eff}, 1+0.5s_{\rm eff}$ for these two type of companion. Thus with $s_{\rm eff} = 0.3$ we find from (32) maximum radii $r_t(\mathrm{ms}) = 1.036, r_t(\mathrm{g}) = 1.195$ for main–sequence and (sub)giant companions respectively ($\nu = 5, -3$). Physically this happens because upon expansion the nuclear luminosity of a main–sequence star decreases, whereas the luminosity generated by a giant does not depend on the radius. Thus assuming that the stars remain on the Hayashi line, a giant must expand until the unblocked area equals its original surface area, while a main sequence star finds a new irradiated equilibrium by expanding and simultaneously reducing its nuclear luminosity. Since $x_U = 1 + p(x_U, r)$, the radius (32) ($p = 0$) has $x_U = 1$ with $s_{\rm eff} = s$, while the radius at which x_U and x_L are equal differs from this only by terms $\sim [f\rho(\nu+5)]^{-1}$. We can then show from equation (31) that x_t is never very large, typically $\sim$ a few times the adiabatic rate.

We can also make some general statements about the properties of the other critical curve $\dot{r} = 0$. All physically plausible $p(r, x)$ must be such that under no mass transfer and no illumination, the star remains at its equilibrium radius, implying $p(1, 0) = 0$. Therefore from equation (12) one sees that the critical curve $\dot{r} = 0$ must go through the point $r = 1, x = 0$. The slope of this curve at that point is also positive, but smaller than the slope of the $\dot{x} = 0$ curve at slightly larger r if a fixed point with $x_0 > 0$ exists. This is obvious from geometrical arguments, but can also be shown explicitly.

A typical limit cycle is shown in Fig. 1, where we have stretched the r variable and exaggerated the separation between the two critical curves for the sake of clarity. Given that the $\dot{r} = 0$ curve intersects the r-axis at $r = 1$, the entire cycle satisfies $r > 1$, i.e. the star is always somewhat oversized. The critical curves cross at the unstable fixed point (r_0, x_0). The four points labelled ABCD along the cycle identify the locations at which the phase point crosses critical curves. These naturally divide the cycle into four phases which we discuss in turn. At point A the mass transfer reaches its peak value $x_A(-\dot{M}_2)_{\rm ad}$ and we have maximum contact: $R_2 - R_L \approx H \ln{(x_A/x_0)}$. We can estimate x_A from the fact that A lies almost vertically above the point where $x_L = 0$. From (28, 30) we have $x_A \approx f\rho s$. In physical units this rate is

$$(-\dot{M}_2)_{\rm max} \approx x_A \frac{M_2}{(\zeta_s - \zeta_{\rm R})t_{\rm dr}} = \frac{sM_2}{(\zeta_s - \zeta_{\rm R})t_{\rm ce}} \;, \tag{33}$$

where $t_{\rm ce}$ is the timescale for thermal relaxation of the convective envelope, which can be significantly shorter than $t_{\rm KH}$. At point B the companion is very close to its maximum size, while the binary orbit has expanded so that $R_2 \approx R_L \approx r_t R_e$. The degree of overfilling of the Roche lobe has been reduced to $R_2 - R_L \approx H \ln{(x_t/x_0)}$. The stellar expansion rate $\dot{R}_2/R_2 = t_{\rm nuc}^{-1}$ is now too slow compared with that of the lobe to sustain the high mass transfer rate which in turn drives the radius expansion. (This is inevitable since the transfer rate cannot indefinitely remain above the secular mean driven by nuclear expansion and angular momentum losses.) Thus the companion rapidly loses contact and the mass transfer drops very sharply, while the star shrinks back towards its equilibrium radius. At point C minimum mass transfer is reached because the system is maximally detached, with $R_2 - R_L \approx -(r_t - 1)/\epsilon$, so that x is essentially zero in the low state. At this point $\dot{R}_2$ is again very close to zero, and nothing will happen until combined effects of nuclear evolution and angular momentum losses bring the system close to contact again. At D the secondary is expanding slightly ($\dot{R}_2/R_2 = \dot{R}_e/R_e$) so that $\dot{r} = 0$. The companion radius R_2 is now within a few scale heights of R_L. This raises the transfer rate, making the companion expand more rapidly under irradiation, which in turn increases the transfer rate, so that the cycle restarts.

We can also estimate the timescales for the different phases of the cycle and evaluate the total mass transferred in a cycle. We estimate the rise time by assuming that the mass transfer initially increases because the thermal imbalance due to irradiation forces the secondary into deeper contact. The characteristic rate of radial expansion when a fraction s is fully blocked is $\mathrm{d}\ln R_2/\mathrm{d}t \approx s/t_{\rm ce}$.

Therefore the rise time is approximately the time required to expand by $\ln(x_A/x_0)$ scale heights

$$t_{DA} \approx \frac{\ln(x_A/x_0) H}{R_2} \frac{t_{\rm ce}}{s} \qquad \text{or} \qquad \tau_{DA} \approx \frac{\ln(x_A/x_0)}{x_A} \,, \tag{34}$$

where we have used our estimate of $x_A = sf\rho$ to obtain the final expression. During the time t_{AB} spent on the high branch, the rate of expansion of the secondary decreases monotonically from the maximum rate estimated above, which yields the peak mass transfer rate x_A, until $\mathrm{d}\ln R_2/\mathrm{d}t = 1/t_{\rm nuc}$. At that point (B) we have $\dot{r} = 0$ and the expansion rate falls below the driving rate so that the system detaches, going rapidly into a low state. We adopt the following ansatz for the radius as a function of time

$$R_2(t) = R_A + (R_B - R_A)(1 - e^{-t/T_+}) \,. \tag{35}$$

Equating $\mathrm{d}\ln R_2(0)/\mathrm{d}t = s/t_{\rm ce}$ and $\mathrm{d}\ln R_2(t_{AB})/\mathrm{d}t = 1/t_{\rm nuc}$, we obtain both the characteristic radial expansion timescale T_+ and the time t_{AB} spent on the high branch

$$T_+ \approx \frac{(r_t - 1)}{s} t_{\rm ce} \sim \frac{t_{\rm ce}}{\nu + 5} \qquad \text{or} \qquad \tau_+ \approx \frac{r_t - 1}{\epsilon x_A} \tag{36}$$

and

$$t_{AB} \approx \frac{(r_t - 1)}{s} t_{\rm ce} \ln(x_A/r_t) \sim \frac{t_{\rm ce}}{\nu + 5} \ln(x_A/r_t) \qquad \text{or} \qquad \tau_{AB} \approx \frac{r_t - 1}{\epsilon x_A} \ln(x_A/r_t) \,, \tag{37}$$

where we have taken $R_A \approx R_e$ and $R_B \approx r_t R_e$. As soon as the system detaches, irradiation ceases, and the companion contracts rapidly while the orbit and Roche lobe remain at the size attained at the end of the high state. The contraction is even more rapid than the expansion because the star is more luminous. One can show that the characteristic thermal contraction time scale is

$$\tau_- \approx (1 - s)^{3/(\nu+5)} \tau_+ \,, \tag{38}$$

leading to

$$t_{BC} \approx \frac{r_t - 1}{r_t^3} \frac{t_{\rm ce}}{s_{\rm eff}} \ln \frac{r_t^2 s_{\rm eff} t_{\rm dr}}{t_{\rm ce}} \qquad \text{or} \qquad \tau_{BC} \approx \frac{(r_t - 1) t_{\rm ce}}{r_t^3 \epsilon s_{\rm eff} t_{\rm dr}} \ln \frac{r_t^2 s_{\rm eff} t_{\rm dr}}{t_{\rm ce}} \,. \tag{39}$$

Clearly this effect is more pronounced in giant companions than in main–sequence secondaries, for reasons that have already been mentioned. In a few times τ_- (i.e. typically a time $\lesssim 0.5 t_{\rm ce}$) the mass transfer formally reaches a minimum value $x_C \approx 0$ and a long detached (low) state now follows while the driving tries to bring the system back to contact. The time spent in the low state is thus dominated by the time t_{CD}

$$t_{CD} \approx (r_t - 1) t_{\rm dr} \sim \frac{s}{\nu + 5} t_{\rm dr} \qquad \text{or} \qquad \tau_{CD} \approx \frac{(r_t - 1)}{\epsilon} \,. \tag{40}$$

The total mass transferred during a cycle can now be estimated as $\Delta M_2 \approx x_A (-\dot{M}_2)_{\rm ad} T_+$, which yields the simple – with hindsight perhaps obvious – result

$$\Delta M_2 \approx (-\dot{M}_2)_{\rm ad} (r_t - 1) t_{\rm dr} = \frac{r_t - 1}{\zeta_s - \zeta_R} M_2 \approx \frac{s_{\rm eff}}{(\zeta_s - \zeta_R)(\nu + 5)} M_2 \,. \tag{41}$$

Hence the total cycle time $t_{\rm cycl} \simeq \Delta M_2/(-\dot{M}_2)_0$ is

$$t_{\rm cycl} \simeq \frac{r_t - 1}{x_0}\, t_{\rm dr} \qquad \text{or} \qquad \tau_{\rm cycl} \approx \frac{(r_t - 1)}{\epsilon x_0}\ . \tag{42}$$

Thus irradiated main–sequence stars ($\nu = 5 - 6$) transfer at most a few percent of their mass per cycle. In contrast giants ($\nu = -3$) transfer a significant fraction $\sim s$ of their total mass M_2 in the high state, which may amount to most of the convective envelope. Since $t_{\rm ce}$ is also much shorter for giants we expect that if the irradiation instability is allowed to grow unchecked in such systems it will produce accretion rates which are super–Eddington in LMXBs. The resulting common–envelope evolution would probably lead to the formation of an ultrashort–period binary. Clearly the irradiation instability must be quenched in observed LMXBs with evolved companions. In Section 7 we discuss ways in which this can happen. For reference we collect together the analytic expressions for the various properties of the limit cycle in Table 1.

6. NUMERICAL RESULTS

We have integrated the evolution equations (11, 12) from arbitrary initial states for a variety of parameter choices. In this section we present a few examples and compare them with the analytic estimates given in the previous section. The values quoted in the text are those obtained by numerical integration, with the corresponding analytic estimate in brackets. The analytic estimates for peak rates, rise times, and maximum expansion radius are in all cases calculated in very good agreement with numerical results. In general we integrated the equations for several cycles (3-6) and noted that the first outburst is usually somewhat untypical (slightly higher for the same radii and a higher peak rate) because of initial conditions, whereas later outbursts are virtually identical. We therefore quote values taken from later outbursts.

Fig. 2 shows a case with core mass $M_c = 0.15{\rm M}_\odot$, the lowest reasonable value for which the approximations used in Section 3 are still valid. We have also taken $s = 0.5$, which is perhaps unrealistically large unless there is significant scattering from a disc corona or similar structure. The luminosity and radius of the companion are at the lower end of the subgiant range and therefore the instability is weakest. Nevertheless a very large amplitude outburst results, with a peak transfer rate $x_A = 152.8$ (154.9) which is attained rapidly, in $\tau_{DA} = 0.032$ (0.033). The companion continues to expand in the high state until the turning point is reached at $r_t = 1.41421$ (1.41421). The duration of the high state can be read off the graph directly and is $\tau_{AB} = 8.1$ (12.5). While the behaviour of r as shown in Fig. 2 appears to obey equation (35), closer examination shows that the expansion phase is actually faster than exponential while the contraction phase is slower than the assumed exponential. Nevertheless we have estimated the characteristic radial expansion and contraction timescales graphically obtaining $\tau_+ = 2.4$ (2.67) and $\tau_- = 1.0$ (0.95). Despite the fact that equation (35) holds only approximately, the expressions based on it are better than order of magnitude estimates. For the case shown, the total duration of the cycle is 415.9 and the duration of the low state is $\tau_{CD} \approx 407.8$ (414.2).

Figure 3 shows another case with a higher core mass $M_c = 0.25\mathrm{M}_\odot$ and $s = 0.3$, appropriate for illumination by a point source. The instability in this case is more violent, with shorter rise times $\tau_{DA} = 0.0023$ (0.0024) and higher peak rates $x_A = 3326$ (3609), but a smaller turning radius $r_t = 1.19529$ (1.19523). The total duration $\tau_{AB} = 0.45$ (0.43) of the high state is relatively short. The characteristic e-folding times for radial expansion $\tau_+ = 0.051$ (0.054) and contraction $\tau_- = 0.04$ (0.031) are also relatively shorter because of the higher luminosity. The analytic estimates for the properties of the radial variations during the limit cycle are even more accurate than in the case in Fig.2, because the neglected terms $\sim (f\rho s)^{-1}$ are still smaller here. The total duration of the cycle is 188.6 and the low state lasts for $\tau_{CD} \approx 188.1$ (195.2).

7. THE IRRADIATION INSTABILITY IN LOW MASS BINARIES

We can now discuss the application of the theory developed here to various types of close binary encountered in nature. The only restriction is that the companions must have a significant convective envelope and thus a low mass $M_2 \lesssim 1.5\mathrm{M}_\odot$. The instability criterion implying cycles given in (26) can be rewritten as

$$f\rho s > \frac{x_0}{r_0^3}\frac{x_c}{x_0}\cosh^2\left(\frac{x_0}{x_c}\right) . \tag{43}$$

Here the factor $x_0/r_0^3 \sim 1$ does not vary much, whereas $f\rho s$ is mainly sensitive to the type of companion and the mechanism driving the binary evolution, while $\xi = x_0/x_c$ depends on both the accretor and donor type. In Fig. 4 we plot x_0/x_c along the abscissa (the compact object axis) and $f\rho s$ along the ordinate (the companion axis). Changing the type of companion causes displacements along both axes, whereas changing the primary causes only horizontal displacements. The stability/instability boundary plotted is simply $f\rho s = \xi^{-1}\cosh^2\xi$. The locations of various possible evolutionary sequences for CVs and LMXBs are also shown on Fig. 4. Changing s by screening or scattering causes purely vertical displacements since ξ is not affected: clearly for any binary there is a value of s below which mass transfer is stable. Within the limitations of the simple theory developed here (i.e. the form chosen for $p(r,x)$) the results displayed on Fig.4 show the following:

1. CVs above the period gap and above a certain period (or companion mass) can be unstable, depending on the value of η (see Paper I). CVs below the gap are stable.

2. Long period CVs with companions having small core masses are stable, whereas companions with larger core masses likely to have even longer orbital periods are unstable. A detailed analysis shows that GK Per and V1017 Sgr are unstable if $\eta \gtrsim 0.08$ and 0.04 respectively.

3. Short–period LMXBs with main sequence or partially evolved companions are stable because they are so strongly irradiated that they have reached saturation ($x_0 >> x_c$). Thus variations in x do not cause radius variations, eliminating the feedback necessary for instability.

4. Long period LMXBs with (sub)giant companions are unstable: the larger the core mass and the smaller the total companion mass, the more violent the instability.

The irradiation instability may well cause the formation of ultrashort–period systems (e.g. the AM CVn's) from long–period CVs and LMXBs. However, since the rise to the high state is so rapid it is extremely improbable that we currently observe any long–period LMXB undergoing cycles. We must therefore consider ways of quenching the instability in these systems. The most obvious possibility is screening of the companion from the irradiation, which is the basic cause of the instability. Screening may well result from the extensive disc coronae inferred in LMXBs (e.g. White & Mason, 1985). Formally we can consider this possibility by decreasing s in our simulations. As can be seen from equation (31) the effect of a small s is to lower the high branch and thus reduce the amplitude of the cycle in x. Since the lower branch remains unaffected, the turning radius and hence the radial amplitude will also be reduced. This suggests that screening could reduce the amplitude of the cycle and increase the frequency of outbursts, because it will take less time to drive the system into contact again once it has detached following an outburst. However this argument applies only to a fixed s. If $s(x)$ is itself a function of the instantaneous mass transfer rate, as a result of a varying geometrical thickness of the accretion disk or varying optical depth through the (out)flow, a more gradual transition occurs. For example, if screening results in a rapid reduction of s beyond some critical $x_{\rm scr}$, the amplitude of the cycle in x is reduced, saturating somewhere close to $x_{\rm scr}$, whereas the radial amplitude remains large; thus the outburst does not recur any sooner than in the unscreened case. We have performed some numerical experiments to simulate these effects and verify the above statements. These simulations and the discussion above imply that if $x_{\rm scr} > x_t$, the radial amplitude of the cycle and recurrence time are not significantly different from the unscreened case. However, if $x_{\rm scr} < x_t$, then both the radial amplitude and the duration of the low state are reduced. Also the duration of the high state and the amount of mass transferred per cycle are decreased. Clearly if $x_{\rm scr}$ is reduced to $\sim x_0$ we will find that the cycles disappear altogether. Thus efficient screening can either eliminate the cycles entirely or render them relatively harmless as far as the binary evolution is concerned.

While screening must play a role in stabilizing some systems against the irradiation instability, a second way of quenching the instability appears to be more common. This mechanism uses the fact that the companion swells only when its own intrinsic luminosity is blocked by the irradiating flux, and that the blocking effect saturates once the latter is comparable with the intrinsic flux. A variable accretion rate, as seen in e.g. soft X–ray transients, severely reduces the efficiency of irradiation in expanding the companion: the very high irradiating flux during outbursts has no more effect than a much weaker value, while the star can cool between outbursts. We might thus expect a highly modulated accretion rate with a duty cycle $d << 1$ to mimic irradiation by a steady accretion rate a factor d smaller. This expectation is largely fulfilled, as the following simple calculation shows.

We assume the dimensionless accretion rate to vary periodically in time over $t_{\rm rec}$ as

$$x_{\rm acc} = x_h, \qquad 0 < t \le t_h, \qquad = x_l, \qquad t_h < t \le t_{\rm rec}. \tag{44}$$

Mass conservation requires that the dimensionless transfer rate obeys

$$x = dx_h + (1-d)x_l = x_h\left[d + \frac{1-d}{A}\right] \tag{45}$$

where $d = t_h/t_{\rm rec}$ is the duty cycle and $A = x_h/x_l$ the amplitude of the accretion rate variation. The reaction of the companion to this intermittent irradiation is governed by the thermal relaxation function (27), which now becomes

$$p = -f\rho\,\left\{\left[1 - s\,\tanh\left(\frac{x}{x_c}\frac{A}{d(A-1)+1}\right)\right]r^3 - r^{-(\nu+2)}\right\}, \qquad 0 < t \le t_h\ , \tag{46}$$

and

$$p = -f\rho\,\left\{\left[1 - s\,\tanh\left(\frac{x}{x_c}\frac{1}{d(A-1)+1}\right)\right]r^3 - r^{-(\nu+2)}\right\}, \qquad t_h < t \le t_{\rm rec}\ . \tag{47}$$

Now assuming that the cycle time $t_{\rm rec}$ is $<< t_{\rm ce}$, we can define a mean value

$$< p >= \frac{1}{t_{\rm rec}}\int_0^{t_{\rm rec}} p(x,r){\rm d}t\ . \tag{48}$$

Performing the integration, we can compute the derivative $< p >_x$ which governs the stability of the fixed point (x_0, r_0). If $x_h >> x_l$, i.e. $A \to \infty$, as is characteristic of soft X–ray transients and dwarf novae, we have

$$< p(x_0, r_0) >_x = \frac{f\rho s r_0^3}{x_c}{\rm sech}^2\left(\frac{x_0}{dx_c}\right)\ , \tag{49}$$

and the criterion for instability $< p(x_0, r_0 >_x > 1$ can be written as

$$f\rho s > \frac{x_0}{r^3}\left(\frac{x_c}{x_0}\right)\cosh^2\left(\frac{x_0}{dx_c}\right)\ . \tag{50}$$

This criterion is very similar to the earlier one (43) assuming steady accretion, to which it of course reduces as $d \to 1$. For $x_0/dx_c \lesssim 1$ the two criteria are identical. Thus on Fig. 4 the stability/instability boundary for $d < 1$ is given simply by sliding the $d = 1$ curve parallel to itself along the asymptote for small x_0/x_c, by a displacement of $-\log d$ in x_0/x_c. We may thus draw a further conclusion from Figure 4:

5. Typical soft X–ray transient duty cycles $d \lesssim 10^{-2}$ are probably enough to stabilize most LMXBs with evolved companions against the irradiation instability.

By contrast, extremely short duty cycles $d \lesssim 10^{-4}$ would be required for dwarf nova outbursts to stabilize CVs with evolved secondaries. We note that most LMXBs with periods $\gtrsim 1$ d are transient (King, Kolb & Burderi, 1996), and indeed this holds for a very large fraction of long–period systems also (King, Kolb & Burderi, 1996; King et al., 1996b). We shall consider the application of the stability criteria to individual systems in a future paper.

8. CONCLUSIONS

We have shown that irradiation of an evolved low–mass companion in LMXBs and CVs can drive mass transfer cycles. These cycles do not need the intervention of any further effect, unlike the case of main–sequence companions (Paper I), where a modest increase in the driving angular momentum loss rate is required in the high state if cycles are to occur in many cases. The cycles with evolved companions are also considerably more violent than in the main–sequence case. This is a direct consequence of two facts. First, the nuclear luminosity of an evolved star is insensitive to the stellar radius, so that blocking of the intrinsic stellar flux by irradiation requires the star to expand so as to maintain the same unblocked area. This leads to much larger expansions than in the main–sequence case, where the nuclear luminosity drops sharply as the star expands. Second, the ratio $t_{\rm dr}/t_{\rm ce} = f\rho$ of driving to thermal timescales is much larger in evolved stars than on the main sequence, making the expansion very rapid. In the high state an evolved star would lose a significant fraction of its total envelope mass on a thermal timescale.

In a CV with a low core mass, the implied accretion rate would probably turn the system into a supersoft X–ray source. In CVs with higher core masses, the nuclear burning causes the white dwarf to develop an extensive envelope, while in long–period LMXBs, the high state accretion rates greatly exceed the Eddington limit. If the instability is not quenched all these systems would undergo a common–envelope phase. They may merge entirely, or reappear as ultrashort–period systems like AM CVn (for white dwarf primaries), or helium–star LMXBs, or detached systems with low–mass white dwarf companions. However, there are at least two ways in which the instability can be quenched and the systems (particularly LMXBs) stabilized: shielding of the companion by e.g. an extensive accretion disc corona, and intermittent accretion. The typical duty cycles $d \lesssim 10^{-2}$ observed in soft X–ray transients are short enough to stabilize them, while observed dwarf nova duty cycles are unable to stabilize CVs with evolved companions.

Although both means of stabilization seem to occur in nature, it is clear that the irradiation instability is so violent that it must play a major role in any discussion of the evolution of CVs and LMXBs with evolved companions: the systems must somehow stave it off or evolve catastrophically. We shall consider some of the observational consequences in a future paper.

JF thanks the Max–Planck–Institut für Astrophysik for warm hospitality during a productive stay in June–August 1996. This work was partially supported by the U.K. Science and Engineering Research Council (now PPARC) and by NASA grant NAG5-2777 to LSU. ARK acknowledges support as a PPARC Senior Fellow, and the warm hospitality of the MPA.

REFERENCES

Hameury, J.-M., & Ritter, H. 1996, A&A, submitted

King, A.R., 1988, QJRAS 29, 1

King, A.R., Frank, J., Kolb, U., & Ritter, H. 1995, ApJ, 444, L40

King, A.R., Frank, J., Kolb, U., & Ritter, H. 1996a, Paper I, ApJ, 447, in press

——— 1996b, ApJ, submitted

King A.R., Kolb U., & Burderi, L., 1996, ApJ 464, L127

King, A.R., & Kolb, U. 1996, ApJ, submitted

Kippenhahn, R. & Weigert, A., 1990, Stellar Structure and Evolution, (Berlin: Springer-Verlag), p. 226

Orosz, J.A., & Bailyn, C.D. 1996, ApJ, in press

Refsdal, S. & Weigert, A., 1970, A&A, 6, 426

Ritter H., Zhang Z., & Hameury J.M., 1996a, in: Cataclysmic Variables and Related Objects, IAU Coll. 158, A. Evans, J.H. Wood (Eds.), Kluwer, in press

Ritter H., Zhang Z., & Kolb U., 1996b, in: Compact Stars in Binaries, IAU-Symp. 165, J. van Paradijs et al. (eds), (Dordrecht: Kluwer), p. 65

Warner B., 1995, Cataclysmic Variable Stars (Cambridge: Cambridge University Press)

Webbink, R.F., Rappaport, S., & Savonije, G.J., 1983, ApJ, 270, 678

This preprint was prepared with the AAS LaTeX macros v4.0.

Table 1: **Characteristic Properties of the Limit Cycle**

Parameters

$t_{\rm dr} = (1/t_{\rm nuc} + 2/t_J)^{-1}$	driving timescale
$t_{\rm ce} = f^{-1} t_{\rm KH}$	thermal timescale of the convective envelope
$\zeta_s = (\partial \ln R_2/\partial \ln M_2)_s$	adiabatic mass radius exponent
$\zeta_e = (\partial \ln R_2/\partial \ln M_2)_e$	thermal equilibrium mass radius exponent
$\zeta_R = (\partial \ln R_{\rm L}/\partial \ln M_2)$	Roche lobe mass radius exponent
$\epsilon = H/R_{2,e}$	photospheric scale height in units of equlibrium radius
$\nu = \begin{cases} 5-6 & \text{MS donors} \\ -3 & \text{giant donors} \end{cases}$	$(-\nu - 3)$ is the radius exponent of the nuclear luminosity
$s_{\rm eff} = s\ \tanh(x_t/x_0) \simeq s \simeq 0.3$	effective blocked surface fraction

Characteristic Properties in the limit	$s_{\rm eff} t_{\rm dr}/t_{\rm ce} \gg 1$
in physical units	in dimensionless form
$(-\dot M_2)_0 = \dfrac{M_2}{\zeta_e - \zeta_{\rm R}} \dfrac{1}{t_{\rm dr}}$	$x_0 = \dfrac{\zeta_s - \zeta_{\rm R}}{\zeta_e - \zeta_{\rm R}}$
$(-\dot M_2)_A \approx \dfrac{M_2}{\zeta_s - \zeta_{\rm R}} \dfrac{s_{\rm eff}}{t_{\rm ce}}$	$x_A \approx \dfrac{s_{\rm eff} t_{\rm dr}}{t_{\rm ce}}$
$R_{2,t} \equiv R_{2,B} \approx (1 - s_{\rm eff})^{-1/(\nu+5)} R_e$	$r_t \equiv r_B \approx (1 - s_{\rm eff})^{-1/(\nu+5)}$
$\Delta M_2 \approx \dfrac{r_t - 1}{\zeta_s - \zeta_{\rm R}} M_2$	$\dfrac{\Delta M_2}{M_2} \approx \dfrac{r_t - 1}{\zeta_s - \zeta_{\rm R}}$
$t_{AB} \approx \dfrac{r_t - 1}{s_{\rm eff}}\, t_{\rm ce}\, \ln \dfrac{s_{\rm eff} t_{\rm dr}}{r_t t_{\rm ce}}$	$\tau_{AB} \approx \dfrac{r_t - 1}{\epsilon\, x_A}\, \ln \dfrac{x_A}{r_t}$
$t_{BC} \approx \dfrac{r_t - 1}{r_t^3}\, \dfrac{t_{\rm ce}}{s_{\rm eff}}\, \ln \dfrac{r_t^2 s_{\rm eff} t_{\rm dr}}{t_{\rm ce}}$	$\tau_{BC} \approx \dfrac{r_t - 1}{r_t^3 \epsilon\, x_A}\, \ln r_t^2 x_A$
$t_{CD} \approx (r_t - 1)\, t_{\rm dr}$	$\tau_{CD} \approx \dfrac{r_t - 1}{\epsilon}$
$t_{DA} \approx \dfrac{\epsilon t_{\rm ce}}{s_{\rm eff}}\, \ln \dfrac{s_{\rm eff} t_{\rm dr}}{x_0 t_{\rm ce}}$	$\tau_{DA} \approx \dfrac{1}{x_A}\, \ln \dfrac{x_A}{x_0}$
$t_{\rm cycl} \approx \dfrac{r_t - 1}{x_0}\, t_{\rm dr}$	$\tau_{\rm cycl} \approx \dfrac{r_t - 1}{\epsilon x_0}$

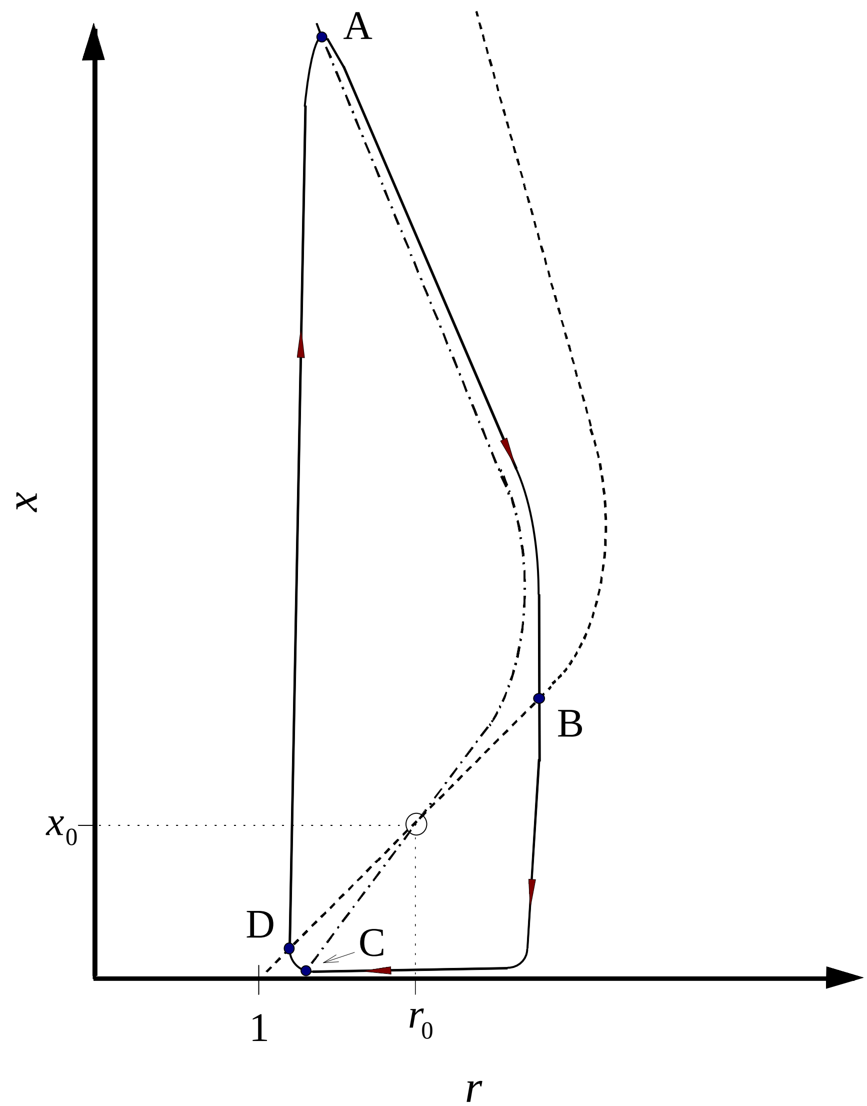

Fig. 1.— Phase plane for the ODE system (11, 12). The two critical curves where $\dot{x} = 0$ (dot-dot-dashed) and $\dot{r} = 0$ (dashed) are shown for a typical $p(r, x)$. These curves intersect at the fixed point (r_0, x_0) and divide the (r, x) plane into four regions in which the motion of the system point is indicated by the arrows. The limit cycle intersects the critical curves at the points ABCD giving the four phases of the cycle discussed in the text: a high state AB during which the companion expands, a moderately rapid contraction phase BC, a long low state CD, and an extremely fast rise DA to peak mass transfer.

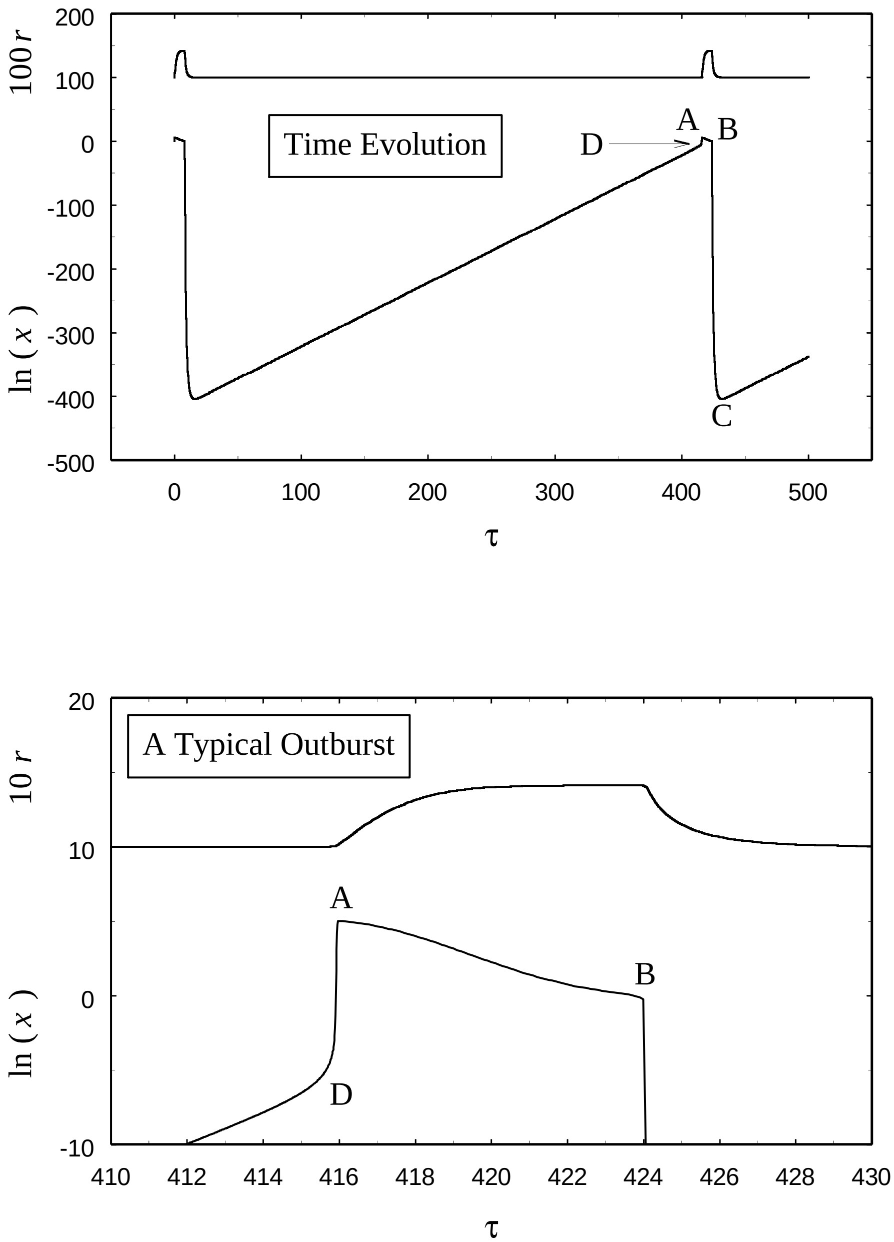

Fig. 2.— The dimensionless mass transfer x and radius r evolution during a typical outburst for a subgiant companion with core mass $M_c = 0.15\mathrm{M}_\odot$ and a large illuminated fraction $s = 0.5$. The calculations assumed a fixed $t_J = 10^{10}$ yr, a neutron star primary with $M_1 = 1.4\mathrm{M}_\odot$ and $R_1 = 10^6$ cm, $M_2 = 0.5\mathrm{M}_\odot$, $\epsilon = 0.001$, $k\eta = 0.01$, $\zeta_s = -1/3$, $\zeta_e = -0.2$, and $\zeta_\mathrm{R} = 2M_2/M_1 - 5/3$.

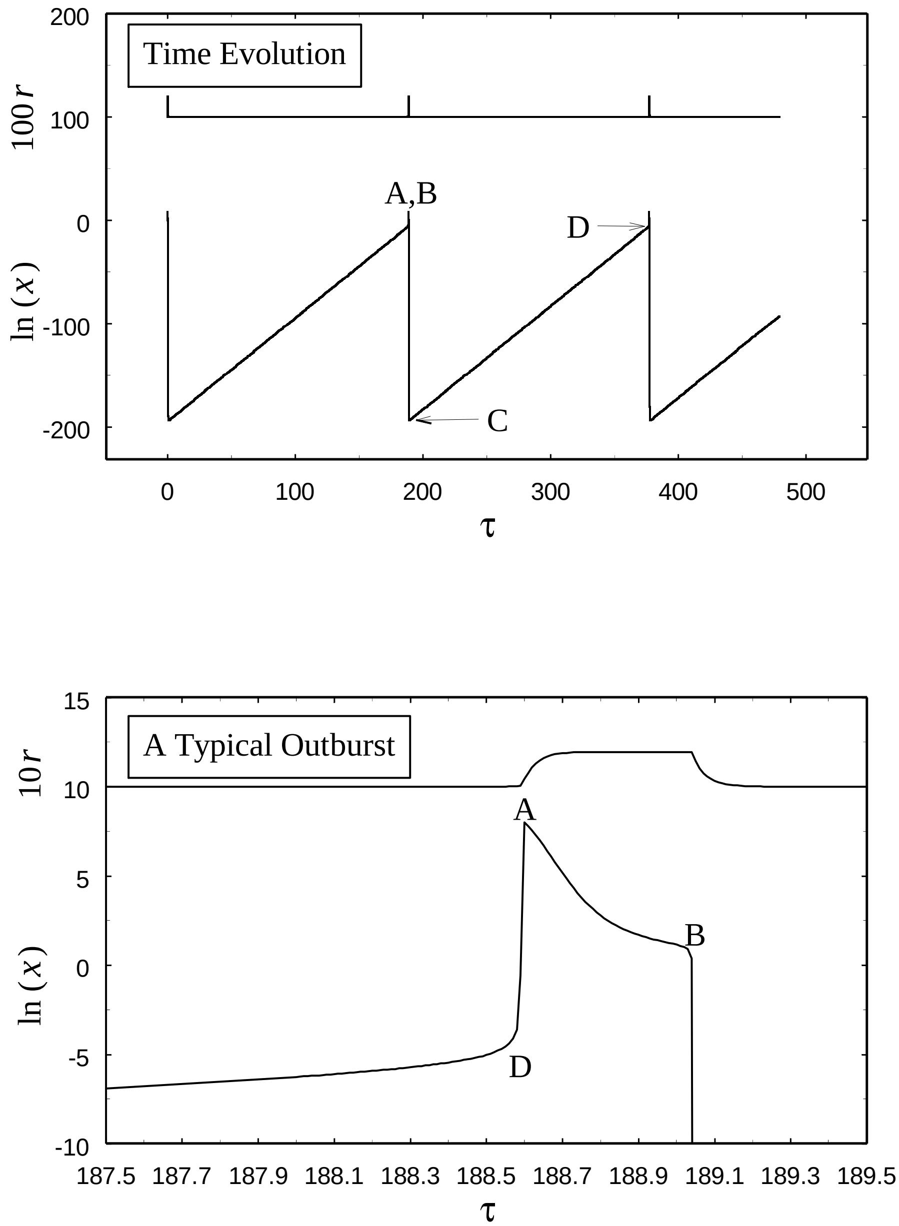

Fig. 3.— The dimensionless mass transfer x and radius r evolution during a typical outburst for a giant companion with core mass $M_c = 0.25\mathrm{M}_\odot$ and an illuminated fraction $s = 0.3$, consistent with a point source. The calculations assumed a fixed $t_J = 10^{10}$ yr, a neutron star primary with $M_1 = 1.4\mathrm{M}_\odot$ and $R_1 = 10^6$ cm, $M_2 = 0.5\mathrm{M}_\odot$, $\epsilon = 0.001$, $k\eta = 0.01$, $\zeta_s = -1/3$, $\zeta_e = -0.2$, and $\zeta_{\mathrm{R}} = 2M_2/M_1 - 5/3$.

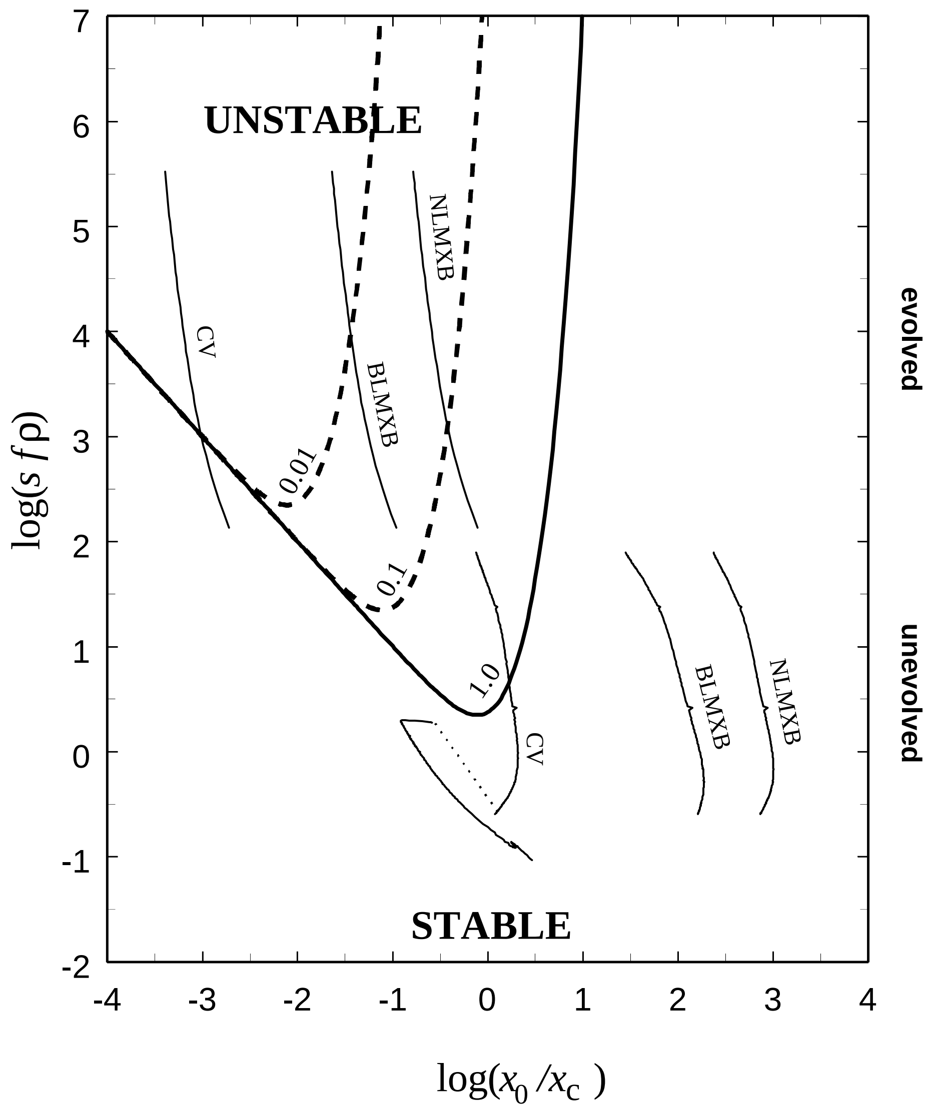

Fig. 4.— The approximate stability boundary given by equation (50) in the $(x_0/x_c, f\rho s)$-plane, for various values of the accretion duty cycle d. Representative evolutionary sequences for different types of low–mass binaries are also indicated. These include black holes, neutron stars and white dwarfs with main–sequence and low–mass giant companions (denoted BLMXB, NLMXB, CV respectively). We took black–hole, neutron star and white dwarf masses $M_1 = 10\mathrm{M}_\odot, 1.4\mathrm{M}_\odot$ and $1.0\mathrm{M}_\odot$, an irradiated fractional area $s = 0.3$, $k\eta = 0.1$ in short–period systems, and $k\eta = 0.01$ in long–period systems. The latter were evolved from an initial core mass $M_{ci} = 0.15\mathrm{M}_\odot$ and total secondary mass $M_{2i} = 0.5\mathrm{M}_\odot$. We see that steady LMXBs with evolved companions are prone to the irradiation instability, while CVs with giant companions are unstable if their core masses are sufficiently large (see text). Typical soft X–ray transient duty cycles $d \lesssim 10^{-2}$ quench the irradiation instability in LMXBs, while typical dwarf nova duty cycles cannot do this for CVs. We stress that while the sequences shown here are representative, the stability or otherwise of any given individual system must be considered in detail.